Human Telomerase Inhibition by Regioisomeric Disubstituted Amidoanthracene-9,10-diones

Philip J. Perry,[†] Anthony P. Reszka,[†] Alexis A. Wood,[†] Martin A. Read,[†] Sharon M. Gowan,[‡] Harvinder S. Dosanjh,[†] John O. Trent,[†,§] Terence C. Jenkins,[†,||] Lloyd R. Kelland,[‡] and Stephen Neidle*[,†]

Cancer Research Campaign Biomolecular Structure Unit and Centre for Cancer Therapeutics, The Institute of Cancer Research, 15 Cotswold Road, Sutton, Surrey SM2 5NG, U.K.

Received July 31, 1998

Telomerase is an attractive target for the design of new anticancer drugs. We have previously described a series of 1,4- and 2,6-difunctionalized amidoanthracene-9,10-diones that inhibit human telomerase via stabilization of telomeric G-quadruplex structures. The present study details the preparation of three further, distinct series of regioisomeric difunctionalized amidoanthracene-9,10-diones substituted at the 1,5-, 1,8-, and 2,7-positions, respectively. Their in vitro cytotoxicity and *Taq* DNA polymerase and human telomerase inhibition properties are reported and compared with those of their 1,4- and 2,6-isomers. Potent telomerase inhibition ($^{tel}IC_{50}$ values 1.3−17.3 μM) is exhibited within each isomeric series. In addition, biophysical and molecular modeling studies have been conducted to examine binding to the target G-quadruplex structure formed by the folding of telomeric DNA. These studies indicate that the isomeric diamidoanthracene-9,10-diones bind to the human telomeric G-quadruplex structure with a stoichiometry of 1:1. Plausible G-quadruplex−ligand complexes have been identified for each isomeric family, with three distinct modes of intercalative binding being proposed. The exact mode of intercalative binding is dictated by the positional placement of substituent side chains. Furthermore, in contrast to previous studies directed toward triplex DNA, it is evident that stringent control over positional attachment of substituents is not a necessity for effective telomerase inhibition.

Introduction

There is increasing evidence that telomerase represents an attractive target for the rational design of new anticancer agents in view of its central role in the control of cellular proliferation.[1,2] Human telomerase is a specialized ribonucleoprotein with an intrinsic RNA component that participates in the maintenance of telomere length.[3] Telomeres, the ends of eukaryotic chromosomes, are characterized by simple G-rich repeating sequences of single-stranded DNA[4] exemplified by the human telomeric sequence 5′-TTAGGG.[5] Telomeres play a vital role in maintaining the stability and integrity of chromosomes and in protecting the ends of chromosomes against aberrant recombination and potential degradation by exonucleases.[6,7] During successive rounds of cell division, the end-replication problem results in telomere shortening and ultimately senescence. As such, the loss of telomeric repeats after each round of cell division has been likened to a 'biological clock' limiting the proliferative life span of normal somatic cells.[8] Telomerase is able to utilize its endogenous RNA template to synthesize telomeric repeats[3] and maintain stable telomere length through an indefinite number of cell divisions. Telomerase activity has been detected in 85−90% of all human cancers and may be essential for cell immortality.[9,10] Consequently, telomerase has been proposed as a potentially highly selective target for the development of a novel class of antiproliferative agents.

G-Rich sequences such as telomeric DNA can associate to form four-stranded inter- and intramolecular guanine quadruplex structures.[11−13] It is well-established that the RNA template region of telomerase requires a linear, nonfolded telomeric DNA primer in order for telomere extension to take place. Thus, the presence of a telomeric G-quadruplex structure results in inhibition of the enzyme.[14,15] We recently described the human telomerase inhibition properties of a series of 1,4- and 2,6-bis(ω-aminoalkanamido)anthracene-9,10-diones (anthraquinones **1** and **2**, Figure 1) and proposed that their activity may be due to their ability to bind to and stabilize G-quadruplex structures.[16,17] This hypothesis was supported by evidence from UV and NMR titration experiments.[16] A porphyrin derivative, tetrakis(*N*-methyl-4-pyridyl)porphine ($TMPyP_4$), has also been shown to bind to G-quadruplex structures[18,19] and inhibit telomerase,[18] possibly via an analogous mechanism.

Previously, we have developed series of structurally related 1,4- and 2,6-bis(ω-aminoalkanamido)anthracene-9,10-diones as DNA-interactive agents. The positional attachment of the ω-aminoalkanamido side chains has been shown to profoundly influence their mode of DNA binding. For example, 1,4-diamidoanthraquinones **1** have been shown to bind to duplex DNA by classical

* To whom correspondence should be addressed. Tel: (+44)-181-643-1675 (direct). Fax: (+44)-181-643-1675. E-mail: steve@iris5.icr.ac.uk.
† CRC Biomolecular Structure Unit.
‡ CRC Centre for Cancer Therapeutics.
§ Present address: Department of Medicine, Division of Hematology/Oncology, University of Alabama at Birmingham, Birmingham, AL 35294.
|| Present address: School of Chemical and Life Sciences, University of Greenwich, Woolwich, London SE18 6PF, U.K.

10.1021/jm981067o CCC: $15.00
Published on Web 10/31/1998

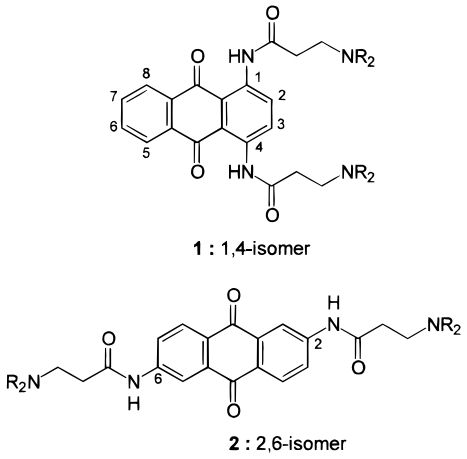

Figure 1. Structures of regioisomeric anthracene-9,10-diones showing substitution at the 1,4- and 2,6-ring positions for **1** and **2**, respectively.

intercalation,[20] whereas their 2,6-disubstituted regioisomers **2** bind by a threading mode, in which the functionalized side chains simultaneously occupy both the DNA major and minor grooves, with intercalation of the planar chromophore.[21] Evidence supporting these two distinct binding mechanisms has been provided by both stopped-flow kinetics[22] and molecular modeling studies.[20,21,23] Knowledge of these distinct modes of binding has since been employed in the identification of compounds that can preferentially bind to and stabilize triplex DNA. For example, molecular modeling, DNA footprinting,[24] and calorimetric[25] techniques have been used to show that 2,6-bis(aminopropionamido)anthraquinones can preferentially bind to and stabilize triplex DNA, whereas their 1,4-regioisomers demonstrate a propensity toward triplex disruption and exhibit favored binding to duplex DNA.

In the present paper we describe the study of further series of regioisomeric 1,5-, 1,8-, and 2,7-bis(aminopropionamido)anthracene-9,10-diones. This has enabled us to address the issue of how, and to what extent, the position of side chain substituents affects telomerase activity. Their in vitro cytotoxicity and *Taq* DNA polymerase and human telomerase inhibition properties are reported and compared with those of their 1,4- and 2,6-regioisomers. In addition, biophysical and molecular modeling studies have been conducted in order to examine binding to the proposed target G-quadruplex structure formed by the folding of human telomeric DNA.

Chemistry

Synthesis of the isomeric bis(aminopropionamido)-anthracene-9,10-diones **9a**−**e**−**18a**−**e** was accomplished as described in Scheme 1. The free-base compounds **9**−**13** were only sparingly soluble in water; hence they were converted into their acid addition salts in order to improve their aqueous solubility.

1,8-Diaminoanthracene-9,10-dione (**4**) was prepared via Gabriel synthesis from 1,8-dichloroanthracene-9,-10-dione in quantitative yield (Scheme 2). 2,7-Diaminoanthracene-9,10-dione (**5**) was obtained by Zinin reduction of 2,7-dinitroanthracene-9,10-dione (**19**), prepared, in turn, by nitration of anthrone (Scheme 3). The salt forms of all compounds were used for subsequent biological and biophysical studies.

Studies

Biological Studies. Compounds **9**−**18a**−**e** were evaluated for in vitro cytotoxicity against three human ovarian carcinoma cell lines (A2780, CH1, and SKOV-3) using the sulforhodamine B (SRB) assay as described previously.[26] Results are presented in Table 1 as the concentrations required to inhibit cell growth by 50% (IC_{50} values). Prior to the evaluation of compounds in a PCR-based telomerase assay, the agents were tested for their ability to inhibit *Taq* polymerase. Compounds were tested at concentrations of 10, 20, and 50 μM, and semiquantitative estimates of *Taq* polymerase inhibition are given (Table 1) for each concentration. The agents were subsequently evaluated for their ability to inhibit human telomerase in a modified cell-free TRAP assay using extracts from the A2780 cell line.[17] Agents were tested at concentrations of 0.5, 1, 5, 10, 20, and 50 μM up to the concentration that *Taq* polymerase inhibition was first observed. Where appropriate, the concentrations required to inhibit telomerase activity by 50% ($^{tel}IC_{50}$ values) are reported in Table 2.

Biophysical Studies. In a previous study[16] we demonstrated telomerase inhibition by a 2,6-diamidoanthraquinone derivative and put forward evidence that the mechanism of action involved binding to and resultant stabilization of G-quadruplex structures. This hypothesis was supported by data from UV and NMR titration experiments that were indicative of a binding mode involving intercalation or base stacking. Isothermal titration calorimetry (ITC) has been used in the present study to demonstrate and then quantitate the interaction of two selected regioisomers (**9e** and **13d**) with the human telomeric sequence d[$AG_3(T_2AG_3)_3$] under conditions shown to favor G-quadruplex formation.[11,18] The resulting binding isotherms, after appropriate correction, were analyzed to give the binding enthalpy ($\Delta H°$), equilibrium binding constant (K_b), and stoichiometry (n). The remaining thermodynamic parameters, $\Delta G°$ and $T{\cdot}\Delta S°$, were derived using standard relationships and are presented in Table 3.

Molecular Modeling Studies. Qualitative molecular modeling studies were conducted with the piperidine derivatives **9a**−**13a** to visualize how different regioisomers might interact with and stabilize the human telomeric G-quadruplex structure. The solution NMR structure of the human telomeric repeat d[$AG_3(T_2AG_3)_3$] G-quadruplex[11] provided an initial starting model. An intercalation site was created between the diagonal T_2A loop and the G-quartet segment of the structure (hereafter referred to as the 5′-AG step). Generated structures for the isomeric piperidine derivatives **9a**−**13a** were minimized, and each, in turn, was docked into the intercalation site. Different positions of the chromophore were systematically evaluated for each regioisomer, with selections made on the basis of maximization of π-electron overlap between the G-quartet, chromophore, and adenine pair. Energy refinement of the resulting G-quadruplex−ligand complexes using molecular mechanics, dynamics, and subsequent mechanics was carried out without the use of positional restraints.

Scheme 1. Synthesis of Isomeric Anthracene-9,10-dione Compounds[a]

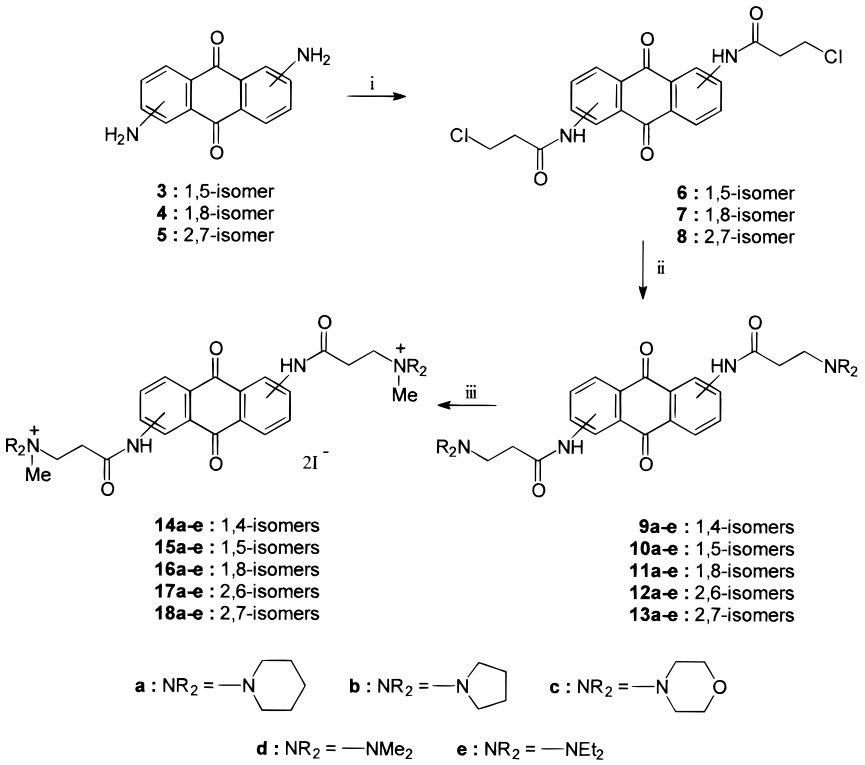

[a] Reagents: (i) $ClCH_2CH_2COCl$/reflux/4 h; (ii) R_2NH/NaI/EtOH/reflux/3 h; (iii) excess MeI/$CHCl_3$/rt/24 h. 1,4-Isomers (**9** and **14**) and 2,6-isomers (**12** and **17**) were prepared as described previously (see refs 19 and 20).

Scheme 2. Synthesis of 1,8-Diaminoanthracene-9,10-dione **4**[a]

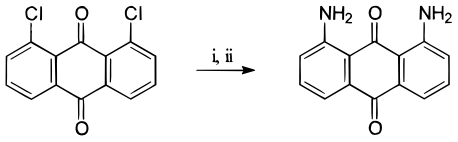

4

[a] Reagents: (i) phthalimide/AcONa/180−200 °C/1 h; (ii) concd H_2SO_4/95 °C/45 min.

Scheme 3. Synthesis of 2,7-Diaminoanthracene-9,10-dione **5**[a]

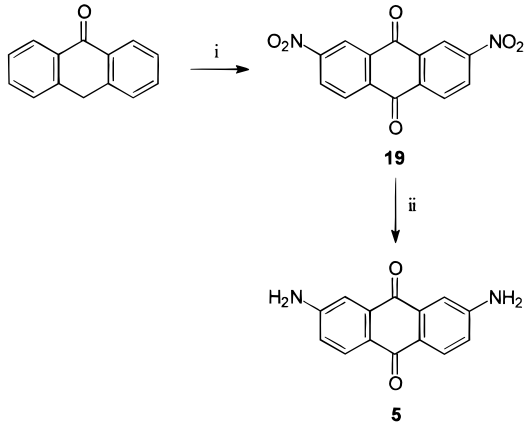

19

5

[a] Reagents: (i) HNO_3/0−5 °C/1−2 h/AcOH/reflux/2 h; (ii) $Na_2S{\cdot}9H_2O$/NaOH/EtOH/reflux/6 h.

Results

The amidoanthraquinones described here exhibit moderate cytotoxicity, with IC_{50} values in the low-micromolar range, against a panel of three ovarian cell lines (A2780, CH1, and SKOV-3). Acid addition salts of the 1,4-, 1,5-, and 1,8-regioisomers (**9**, **10**, and **11**, respectively) were generally more cytotoxic than the 2,6- and 2,7-isomers, **12** and **13**, respectively. The regioisomeric morpholine derivatives (**9c**−**13c**) were found to be the least potent of the compounds studied. The quaternary dimethiodide salts **14**−**18** exhibited broadly similar cytotoxic activities. The 1,4- and 1,5-regioisomeric dimethiodide salts **14** and **15**, respectively, were generally less potent than their corresponding acid addition salts, while the 1,8- and 2,6-isomers (**11** and **16**, and **12** and **17**, respectively) were found to be broadly similar. However, the 2,7-regioisomeric dimethiodides **18** were more cytotoxic than their corresponding acid addition salts.

The majority of compounds examined were relatively ineffective inhibitors of *Taq* polymerase, with little or no inhibition of the enzyme evident at concentrations up to 50 μM. However, three of the 1,4-disubstituted acid addition salts (**9a,b,d**) exhibited significant inhibition at 20 μM with slight inhibition observed at 10 μM. Inhibition of *Taq* polymerase by the 2,6-disubstituted dimethiodides was also observed, with compounds showing either total (**17a,c,e**) or significant (**17b**) inhibition at 20 μM.

The compounds were tested for their ability to inhibit telomerase ($^{tel}IC_{50}$ values) using the TRAP assay up to the concentration at which *Taq* polymerase inhibition was observed. The nucleotide ddGTP, which we have previously shown[17] to be a relatively potent inhibitor of telomerase ($^{tel}IC_{50}$ = 8.6 μM), was used as a positive control. A typical gel pattern arising from a TRAP experiment is shown in Figure 2. Telomeric repeat ladders are seen in the 0.01- and 0.04-μg protein positive

Table 1. In Vitro Cytotoxicity and *Taq* Polymerase Inhibition Data for Isomeric Anthracene-9,10-diones **9**−**18**

		IC_{50} (μM)[a]			*Taq* inhibition[b]		
compd	isomer	A2780	CH1	SKOV-3	10 μM	20 μM	50 μM
9a	1,4	0.29	0.26	2.4	+	++	+++
9b	1,4	0.0025	0.019	0.39	++	+++	+++
9c	1,4	3.7	1.95	21.0	−	−	−
9d	1,4	0.016	0.04	0.36	+	++	+++
9e	1,4	0.2	0.26	1.4	−	−	+++
10a	1,5	0.435	0.42	0.82	−	−	+
10b	1,5	0.32	0.36	0.53	+	++	++
10c	1,5	>25	>25	>25	−	−	−
10d	1,5	0.35	0.37	0.62	−	−	++
10e	1,5	0.32	0.32	0.62	−	−	+
11a	1,8	0.54	1.95	2.35	−	−	+
11b	1,8	0.295	1.28	1.2	−	+	+++
11c	1,8	>25	21.5	>25	−	−	−
11d	1,8	0.33	1.35	1.65	−	−	−
11e	1,8	0.64	5.3	5.2	−	−	−
12a	2,6	1.3	5.9	4.0	−	−	−
12b[c]	2,6	39	49	38	−	−	+++
12c	2,6	>25	14.0	>25	−	−	−
12d	2,6	2.55	1.8	2.9	−	−	+++
12e	2,6	2.35	3.15	3.15	−	−	+++
13a	2,7	0.48	3.15	3.7	−	−	−
13b	2,7	1.2	1.8	2.3	−	−	+++
13c	2,7	5.3	7.5	>100	−	−	−
13d	2,7	2.1	4.4	4.15	−	−	−
13e	2,7	2.1	4.6	7.2	−	−	++
14a	1,4	1.75	4.3	32.5	−	−	−
14b	1,4	1.5	4.5	37	−	−	−
14c	1,4	0.76	1.65	8.5	−	−	−
14d	1,4	2.15	2.0	11.5	−	−	++
14e	1,4	4.25	6.3	>25	−	−	+
15a	1,5	2.0	2.1	8.3	−	−	−
15b	1,5	2.2	2.25	10.0	−	−	−
15c	1,5	1.9	1.8	2.9	−	−	−
15d	1,5	1.7	1.75	5.8	−	−	−
15e	1,5	1.9	2.05	10.0	−	−	−
16a	1,8	0.52	1.12	4.6	−	−	−
16b	1,8	0.6	1.68	5.0	−	−	−
16c	1,8	0.51	0.58	2.6	−	−	−
16d	1,8	0.53	1.4	2.2	−	−	−
16e	1,8	0.55	1.65	4.6	−	−	−
17a	2,6	<1	1.85	2.2	−	+++	+++
17b	2,6	0.56	1.35	2.0	−	++	+++
17c	2,6	1.9	1.7	3.0	−	+++	+++
17d	2,6	2.25	1.9	4.4	−	−	−
17e	2,6	2.1	1.9	6.4	−	+++	+++
18a	2,7	0.18	1.05	2.2	−	−	−
18b	2,7	0.48	1.6	4.7	−	−	++
18c	2,7	0.52	1.1	2.95	−	−	−
18d	2,7	0.44	1.3	4.0	−	−	++
18e	2,7	0.33	1.13	2.0	−	−	++

[a] Concentration required to inhibit cell growth by 50% relative to controls. [b] Key: (+++) total, (++) significant, (+) slight, or (−) no inhibition. [c] Administered as a fine suspension.

Table 2. Telomerase Inhibition Data for Compounds **9a**−**e**−**18a**−**e**

		telomerase IC_{50} values[a] (μM) for substituents $-NR_2$				
compd	isomer	1-piperidinyl (**a**)	1-pyrrolidinyl (**b**)	4-morpholinyl (**c**)	NMe_2 (**d**)	NEt_2 (**e**)
9	1,4	nd	nd	33.5	nd	1.8
10	1,5	2.3	nd	>50	1.3	2.7
11	1,8	3.7	nd	>50	6.4	4.2
12	2,6	4.5	1.8	>50	4.1	3.5
13	2,7	3.1	2.0	≫50	4.7	4.3
14	1,4	11.1	5.0	34.5	7.0	3.1
15	1,5	8.6	8.8	14.0	13.2	16.8
16	1,8	7.8	8.2	10.0	4.4	7.5
17	2,6	nd	nd	nd	17.3	nd
18	2,7	7.8	16.0	16.5	14.5	>20

[a] Concentration required to inhibit telomerase activity by 50% relative to controls; nd, not determined.

control (lanes 2 and 3, respectively), while ladders were not produced either in the absence of telomerase (lane 1) or when heat inactivation of the protein extract was performed (lane 4). A concentration-dependent inhibition of telomerase by **13d** is clearly evident in lanes 5−8 (20, 10, 5, and 1 μM, respectively). Similarly, ladders for ddGTP are presented in lanes 9−12 at the same range of concentrations which show it to be a less potent

Table 3. Thermodynamic Data for Binding of Compounds **9e** and **13d** to G-Quadruplex[a]

compd	n[b]	K_b ($\times 10^4$ M^{-1})	$\Delta H°$ (kcal mol^{-1})	$\Delta G°$ [c] (kcal mol^{-1})	$T{\cdot}\Delta S°$ [d] (kcal mol^{-1})
9e	1.2	7.9 ± 0.9	−5.5 ± 0.2	−6.7	+1.2
13d	1.3	5.1 ± 1.1	−10.1 ± 2.0	−6.4	−3.7

[a] Determined by ITC at 25 °C for the 22-mer sequence $d[AG_3(T_2AG_3)_3]$. We estimate that all energies are within 5−10% of calculated values as no correction was applied for the heats of dissociation of the ligand dimers (see text). [b] Number of molecules bound per G-quadruplex; values ± ≤ 0.2. [c] Free energy of binding was calculated using $\Delta G° = -RT \ln K_b$. [d] The entropy term was calculated using $\Delta G° = \Delta H° - T{\cdot}\Delta S°$.

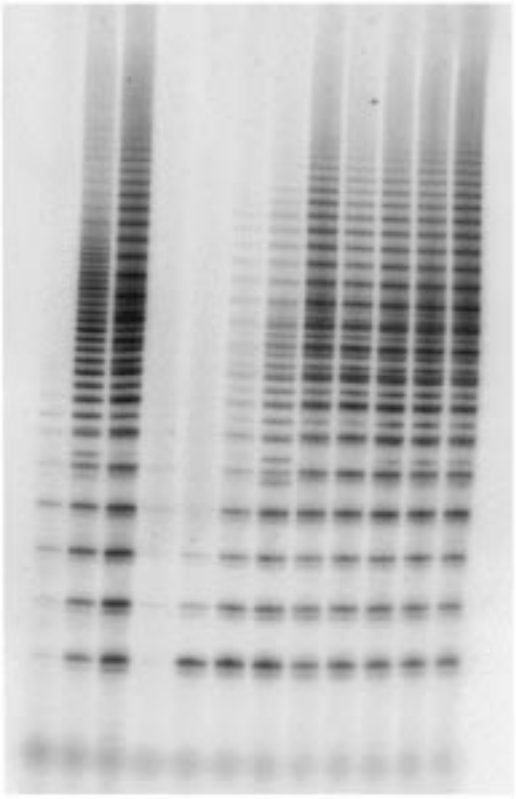

Figure 2. Gel of a TRAP experiment showing telomerase inhibition by **13d** and ddGTP. Lane 1, lysis buffer negative control; lane 2, positive control 0.01 μg of telomerase protein; lane 3, positive control 0.04 μg of protein; lane 4, heat-inactivated negative control; lanes 5−8, **13d** at 20, 10, 5, and 1 μM, respectively; lanes 9−12, ddGTP at 20, 10, 5, and 1 μM, respectively.

inhibitor than **13d**. All of the compounds described, with the exception of the morpholine derivatives **9**−**14c** and compound **18e**, were shown to be effective inhibitors of human telomerase ($^{tel}IC_{50}$ values ranging from 1.3 to 17.3 μM). These values compare favorably with those of previously described small-molecule inhibitors of telomerase.[18,27,28] The diminished activities exhibited by the morpholine acid addition salts may, at least in part, be due to their reduced basicity relative to the other compounds described. Generally, the acid addition salts **9**−**13** were more active than the corresponding quaternary dimethiodide derivatives **14**−**18**. This may be related to accessibility of the charge on the protonated nitrogen.

ITC was used to give direct measurement of the binding enthalpy ($\Delta H°$), which then enabled equilibrium binding constants (K_b), and stoichiometry (n) to be

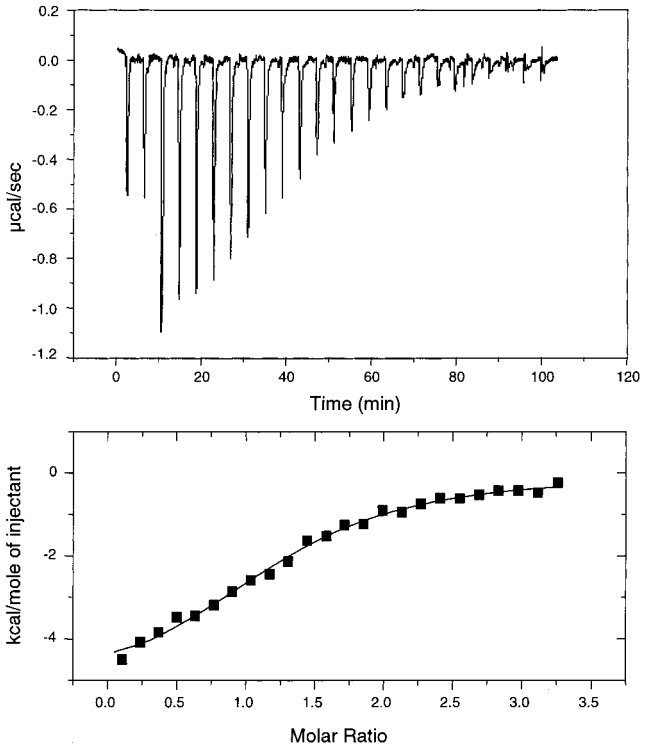

Figure 3. Calorimetric data for the titration of $d[AG_3(T_2AG_3)_3]$ with **9e** determined at 25.00 ± 0.01 °C, showing exothermic binding. The peaks in the upper panel represent the power output associated with each injection of ligand into DNA as a function of time. Integration of these peaks gives the corresponding binding isotherm in the lower panel, for [ligand]:[DNA] ratios of 0 → 3.25:1.

determined. $\Delta G°$ and $T{\cdot}\Delta S°$ were derived using standard thermodynamic relationships. Figure 3 shows the ITC data for the titration of the 22-mer human telomere sequence with **9e**. These data were subsequently corrected for the heats of dilution associated with the addition of ligand into buffer, but not for dissociation of any dimeric species. As described previously,[25] such molecules have dimerization constants K_2 in the order of 3×10^3 M^{-1} at 25 °C, and we would thus expect there to be <5% of free ligand remaining in solution at completion of the titration for these analogous molecules. Fitting of the corrected data using a single-site binding model allows stoichiometry (n), equilibrium binding constant (K_b), and binding enthalpy ($\Delta H°$) to be determined (Table 3).

Both of the regioisomers investigated (**9e** and **13d**) were shown to bind to the G-quadruplex structure with a stoichiometry of 1:1 (within experimental error) and with similar affinity. This is paralleled in the telomerase inhibition activities exhibited by the two compounds (**9e** and **13d**: 1.8 and 4.7 μM, respectively). Examination of the thermodynamic data shows that binding of both isomers is exothermic in nature. Further, the binding enthalpies of both **9e** and **13d** (−5.5 and −10.1 kcal mol^{-1}, respectively) are typical values for DNA binding ligands.[25,29]

Final orientations from the averaged molecular dynamics structures for each regioisomer (**9a**−**13a**) are shown in Figure 4. Figure 4a shows a side view of the 2,6-disubstituted regioisomer **12a** occupying a single intercalation site at the 5′-AG step of the G-quadruplex structure. Figure 4b shows the final orientation of

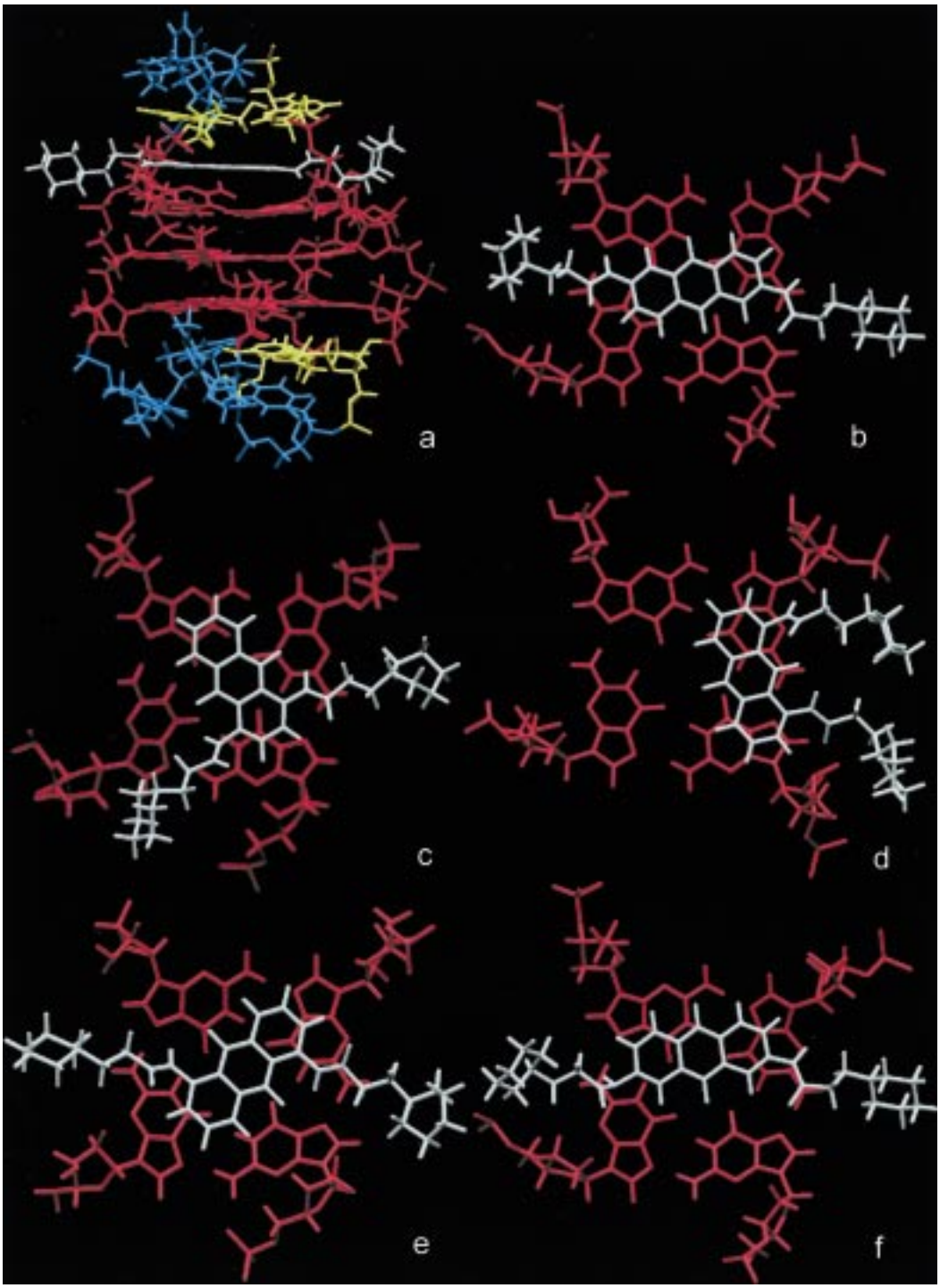

Figure 4. Comparison of binding conformations of the regioisomeric piperidine derivatives **9a**−**13a**. (a) Side view of the 2,6-regioisomer **12a** bound in the 5′-AG step of the human telomeric G-quadruplex structure. (b) 2,6-Regioisomer **12a** viewed from above showing the orientation with respect to the adjacent G-quartet. Similar views are shown for 1,4- (c), 1,8- (d), 1,5- (e), and 2,7- (f) regioisomers (**9a**, **11a**, **10a**, and **13a**, respectively).

compound **12a** viewed from above, with respect to the adjacent G-quartet. Regioisomers **9a** (1,4), **11a** (1,8), **10a** (1,5), and **13a** (2,7) are similarly shown in Figures 4c−f, respectively. Three distinct modes of intercalative binding were established for the five different regioisomeric series. The 2,6-, 1,5-, and 2,7-disubstituted regioisomers were found to adopt a favored threading mode of intercalation in which the two substituent side chains are positioned in opposite grooves of the G-quadruplex structure (Figure 4b,e,f, respectively). Similarly, the most favorable conformation for the 1,4-regioisomer resulted in a threading mode of intercalation, but with the substituent side chains positioned in adjacent grooves (Figure 4c). In contrast, the most favorable conformation for the 1,8-isomer corresponds to a classical mode of intercalation. In this example, the planar chromophore was shown to overlap two of the four guanines of the G-quartet, with both the substituent side chains simultaneously occupying the same groove (Figure 4d). The remaining two guanines of the G-quartet are stabilized by stacking with the adenine pair (not shown). The resultant stabilization

afforded by these compounds is due to a combination of maximization of π-stacking interactions in the intercalation site, electrostatic interactions between the phosphate backbones and the positively charged amine side chains, and nonbonded van der Waals interactions in the G-quartet grooves with side chain atoms.

Discussion

The amidoanthraquinones described here showed only moderate cytotoxicity against a panel of three ovarian cell lines (Table 1) and were typically 2−3 orders of magnitude less potent than the clinically established quinones doxorubicin and mitoxantrone.[17] If telomerase inhibitors such as those described here are to have application as antitumor agents, with telomerase inhibition in tumor cells leading to attrition of telomere length and consequent senescence, then prolonged administration will most likely be necessary as a significant number of rounds of cell division may ultimately be required to produce such an effect. Consequently, to obtain a useful comparative therapeutic index (TI), where TI = $IC_{50}/^{tel}IC_{50}$, conventional cytotoxicity should be minimized with respect to telomerase inhibition. For the compounds examined, Tables 1 and 2 indicate that only the 1,4-isomer **14e** has a TI value greater than 1 (i.e., TI = 1.4) with respect to the A2780 cell line used for the TRAP assay. Interestingly, and without exception, compounds **9**−**18** were consistently less cytotoxic toward SKOV-3 cells than the A2780 cell line (Table 1). Furthermore, approximately half of the agents evaluated were an order of magnitude less cytotoxic to SKOV-3 cells. In contrast, cytotoxicity levels toward CH1 cells were more comparable to those in A2780. Therefore, compound **14e** has a significantly improved therapeutic index (TI > 8) with respect to SKOV-3 cells and hence it would be of interest to further investigate the telomerase inhibitory properties of this compound in vitro using SKOV-3 cells, and in vivo with mice bearing companion SKOV-3 xenografts. As noted for other DNA interactive agents, the reduced levels of cytotoxicity observed against SKOV-3 are probably due to enhanced DNA-damage repair and tolerance mechanisms known to operate in this cell line compared to the other ovarian cell lines in the panel examined.[30]

We have previously established a correlation between the mode and affinity of binding to duplex DNA and resultant biological properties for a series of analogous diamidoanthracene-9,10-diones.[20,21] The binding constants to duplex DNA are comparable to those reported here for binding to G-quadruplex DNA (Table 3). Sheardy and co-workers recently reported,[19] using Scatchard plot analysis, the binding constant for the interaction of $TMPyP_4$ with quadruplexed T_4G_4 as 2.7×10^7 M^{-1}, a value approximately 350−500 times greater than that for the ligands examined here. This result would appear to be somewhat surprising given that the telomerase inhibition of $TMPyP_4$ ($^{tel}IC_{50}$ = 6.5 μM) was shown[18] to be very similar to those of the compounds described in the present study. Further, our results are more in keeping with those reported for the binding of ethidium bromide to quadruplexed T_4G_4 and porphyrin binding to a number of G-quadruplexes, as determined by ITC.[29,31]

The intercalation site for the molecular modeling studies was selected on the basis of evidence from both NMR and biophysical studies.[18,19,29] G-Quadruplexes are known to be extremely stable structures due to favorable $\pi-\pi$-stacking of the G-quartets and the presence of tightly bound potassium or sodium ions. Thus, intercalation between G-quartet planes is unfavorable due to the disruption this would cause to the quadruplex structure. The molecular modeling studies indicate that a number of distinct intercalative modes of binding to this single site within the G-quadruplex structure are possible. These distinct binding modes are dictated by the positional placement of substituent side chains for each isomer, with the exact conformation adopted by the chromophore for any one mode of binding being a result of the maximization of $\pi-\pi$-interactions within the intercalation site. Direct comparison of calculated binding energies for individual G-quadruplex−ligand complexes is inappropriate in the absence of detailed simulations with explicit solvent. However, qualitative evaluation of molecular dynamic trajectories indicates that the diagonal T_2A loop region adjacent to the intercalation site is the most flexible region of the structure, resulting in high mobility during molecular dynamics simulations. This feature, combined with the relatively large aromatic plane of the G-quartet, accounts for the ability of the G-quadruplex structure to associate with these regioisomeric anthraquinones.

In contrast to previous studies[22−25] directed toward triplex DNA in which the positional attachment of substituent side chains was shown to profoundly influence the mode of DNA binding and resultant stabilization, the present study indicates that a stable G-quadruplex−ligand complex is feasible for each regioisomeric series. Furthermore, the finding that potent telomerase inhibition ($^{tel}IC_{50}$ values of 1.3−3.7 μM) was observed within each isomeric series is suggestive of a role for G-quadruplex involvement in the inhibitory activity displayed by these compounds. This insensitivity to positional isomerism is a consequence of the four grooves present in the G-quadruplex structure as opposed to the two and three grooves in duplex and triplex DNA, respectively. We therefore conclude that the positional placement of substituents on the anthraquinone chromophore is of less importance than the nature of the substituents.

The validity of telomerase as an anticancer target has recently been questioned.[32] However, it is now apparent that the initial conclusions based on telomerase 'knockout' mice[32] were premature, and longer-term experiments[33] have shown that telomerase plays an essential role in cell proliferation. In addition, recent antisense experiments with a 2′,5′-tetraadenylate-linked oligonucleotide construct targeted toward the human telomerase RNA have provided further evidence validating telomerase as an anticancer target.[34] Recent evidence also suggests that an alternative mechanism for telomere maintenance may exist in certain yeast, ciliate, and human tumor cell lines.[35] Telomerase inhibitors could well be of major use as selective anticancer drugs, perhaps following conventional debulking therapy. Therefore, compounds such as those described here that inhibit telomerase indirectly by targeting telomeric G-quadruplex structures may also have the potential to impede non-telomerase-mediated pathways for telomere maintenance. As such, the development of small

molecules that selectively bind to and stabilize G-quadruplex structures, and that are noncytotoxic, may enable the development of a new class of clinically useful and highly selective drugs. Furthermore, the recent finding that amidoanthracene-9,10-diones such as those described here are nonmutagenic[36] makes them of particular appeal for potential long-term administration.

Experimental Section

Synthetic Chemistry. Melting points (mp) were recorded on a Leica Galen III hot-stage melting point apparatus and are uncorrected. NMR spectra were recorded at 250 MHz on a Bruker AC250 spectrometer in either Me_2SO-d_6 or $CDCl_3$ solution at 303 ± 1 K using Me_4Si as internal standard. Chemical shift assignments for the 1,5- and 1,8-isomers were determined by ^1H NMR titration experiments conducted with Eu(fod)$_3$ (0−2 mol equiv) and **7** in $CDCl_3$. EI (70 eV), FAB, and high-resolution accurate mass spectra were determined by The School of Pharmacy (University of London, U.K.). Elemental analyses were carried out by Medac Ltd. (Brunel Science Center, Egham, Surrey, U.K.); results for elements indicated by symbols were within ±0.4% of theoretical values. TLC was carried out on silica gel (Merck 60F-254) using $CHCl_3$−MeOH (0−20% MeOH) as eluent, with visualization at 254 and 366 nm. Organic solutions were dried over sodium sulfate. 1,4-Isomers (**9a**−**e** and **14a**−**e**) and 2,6-isomers (**12a**−**e** and **17a**−**e**) were prepared using published procedures.[19,20]

1,8-Diaminoanthracene-9,10-dione, 4. A stirred mixture of 1,8-dichloroanthracene-9,10-dione (41.6 g, 0.15 mol), phthalimide (52.7 g, 0.385 mol), anhydrous sodium acetate (29.6 g, 0.361 mol), and nitrobenzene (77 mL) was heated to 180 °C. Quinoline (25 mL) and copper powder (300 mesh, 0.72 g) were added, and the mixture was heated at 200 °C for 1 h. The reaction mixture was allowed to cool and left to stand overnight. The mixture was filtered, washed with nitrobenzene (3 × 100 mL), ethanol (3 × 100 mL), hot water (3 × 200 mL), ethanol (2 × 100 mL), and ether (2 × 100 mL), and dried to give the intermediate diphthalimide as a pale-yellow/orange solid: mp > 360 °C (56.66 g, 76%). The crude solid (56.0 g) was added to concentrated H_2SO_4 (400 mL) with stirring and the mixture heated at 95 °C for 45 min. The reaction mixture was cooled to 5 °C, and crushed ice (150 g) was slowly added. The mixture was poured onto ice/water (1.5 L) with stirring, and the resulting precipitate was collected by filtration, washed with water until neutral, and dried in vacuo. Recrystallization from ethanol afforded the product as red/purple needles (27.0 g, 98%): mp 270−271 °C (lit.[37] mp 269−270.5 °C); NMR δ (DMSO) 7.15 (2H, dd, J = 8.5 and 1.4 Hz, H-2,7), 7.34 (2H, dd, J = 7.4 and 1.4 Hz, H-4,5), 7.45 (2H, dd, J = 8.5 and 7.4 Hz, H-3,6), 7.86 (4H, br s, NH_2); MS (rel intensity) m/z 238 (100), 210 (12), 181 (7), 154 (8), 119 (9), 91 (7), 77 (8); calcd ([M + 1]$^+$) 239.0821, found 239.0810. Anal. ($C_{14}H_{10}N_2O_2$) C, H, N.

2,7-Dinitroanthracene-9,10-dione, 19. Anthrone (21.25 g, 0.109 mol) was added with stirring to a cooled solution of fuming nitric acid (142 mL) at such a rate as to maintain a reaction temperature of 5 °C. After completion of the addition (ca. 1.5 h), the reaction mixture was allowed to reach ambient temperature. The reaction mixture was added to glacial acetic acid (430 mL) with cooling, lightly stoppered, and allowed to stand at room temperature for 1 week. The resulting precipitate was collected by filtration, washed with glacial acetic acid (3 × 25 mL) and hexane (3 × 25 mL), and dried. The crude solid was suspended in glacial acetic acid (4 L) and heated at reflux until the evolution of nitrous fumes had ceased (ca. 2 h). The mixture was allowed to cool to room temperature and left to stand for 48 h. The resulting precipitate was collected by filtration, washed with glacial acetic acid (3 × 30 mL) and hexane (3 × 30 mL), and dried to give a pale-yellow solid (10.34 g, 32%). Recrystallization from nitrobenzene/glacial acetic acid (1:1 v/v) afforded a pure sample of **19**: mp 290−291 °C (lit.[38] mp 290−291 °C); NMR δ (DMSO) 8.48 (2H, dd, J = 8.4 and 1.4 Hz, H-4,5), 8.71 (2H, dt, J = 8.4 and 1.9 Hz, H-3,6), 8.83 (2H, t, J = 1.9 Hz, H-1,8); MS (rel intensity) m/z 298 (100), 252 (75), 196 (22), 178 (23), 150 (67), 75 (34); calcd (M$^+$) 298.0226, found 298.0240. Anal. ($C_{14}H_6N_2O_6$) C, H, N.

2,7-Diaminoanthracene-9,10-dione, 5. To a stirred suspension of 2,7-dinitroanthracene-9,10-dione (**19**) (9.4 g, 31.5 mmol) in ethanol (340 mL) was added a solution of sodium sulfide nonahydrate (34.1 g, 142 mmol) and sodium hydroxide (13.5 g, 338 mmol) in water (590 mL). The mixture was heated at reflux for 6 h and left to stand overnight. The ethanol was removed in vacuo and the residue cooled to 0−5 °C. The resulting precipitate was collected by filtration, repeatedly washed with water, and dried. Recrystallization from ethanol/water afforded the product as an orange/red solid (7.35 g, 98%): mp 337−338 °C (lit.[39] mp 330−332 °C); NMR δ (DMSO) 6.42 (4H, br s, NH_2) 6.89 (2H, dd, J = 8.5 and 1.5 Hz, H-3,6), 7.23 (2H, d, J = 1.5 Hz, H-1,8), 7.84 (2H, d, J = 8.5 Hz, H-4,5); MS (rel intensity) m/z 239 (35), 176 (26), 154 (24), 136 (100), 106 (31); calcd ([M + 1]$^+$) 239.0821, found 239.0830. Anal. ($C_{14}H_{10}N_2O_2$) C, H, N.

1,5-Bis(3-chloropropionamido)anthracene-9,10-dione, 6. General Acylation Procedure. A suspension of 1,5-diaminoanthraquinone (3.0 g, 12.6 mmol) in 3-chloropropanoyl chloride (60 mL) was heated at reflux for 4 h, until TLC indicated completion of reaction. After cooling to 0−5 °C, the mixture was filtered and the crude solid washed with ether (3 × 50 mL). Recrystallization from DMF−EtOH (4:1 v/v) afforded chloroamide **6** (3.0 g, 57%) as yellow/brown crystals: mp 280−281 °C; NMR δ ($CDCl_3$) 3.04 (4H, t, J = 6.4 Hz, $COCH_2$), 3.95 (4H, t, J = 6.4 Hz, CH_2Cl), 7.82 (2H, t, J = 8.1 Hz, H-3,7), 8.08 (2H, dd, J = 8.1 and 1.0 Hz, H-4,8), 9.16 (2H, dd, J = 8.1 and 1.0 Hz, H-2,6), 12.40 (2H, s, NH); MS (rel intensity) m/z 421 (100), 419 (74), 418 (20), 411 (25), 403 (23), 383 (52), 357 (26), 344 (25), 293 (26); calcd ([M + 1]$^+$) 419.0565, found 419.0575. Anal. ($C_{20}H_{16}N_2O_4Cl_2$) C, H, N, Cl.

1,8-Bis(3-chloropropionamido)anthracene-9,10-dione, 7. 1,8-Diaminoanthracene-9,10-dione (**4**) was treated with 3-chloropropanoyl chloride according to the general acylation procedure to give chloroamide **7** (3.7 g, 70%) as orange crystals: mp 249−250 °C; NMR δ ($CDCl_3$) 3.06 (4H, t, J = 6.5 Hz, $COCH_2$), 3.97 (4H, t, J = 6.5 Hz, CH_2Cl), 7.81 (2H, t, J = 8.5 Hz, H-3,6), 8.08 (2H, dd, J = 8.5 and 1.0 Hz, H-4,5), 9.18 (2H, dd, J = 8.5 and 1.0 Hz, H-2,7), 12.18 (2H, s, NH); MS (rel intensity) m/z 418 (21), 382 (21), 347 (13), 328 (34), 292 (25), 265 (55), 238 (90), 91 (18), 63 (46), 55 (100); calcd ([M + 1]$^+$) 419.0565, found 419.0550. Anal. ($C_{20}H_{16}N_2O_4Cl_2$) C, H, N, Cl.

2,7-Bis(3-chloropropionamido)anthracene-9,10-dione, 8. 2,7-Diaminoanthracene-9,10-dione (**5**) was treated with 3-chloropropanoyl chloride according to the general acylation procedure to give chloroamide **8** (4.33 g, 82%) as a yellow solid: mp 289−290 °C dec; NMR δ (DMSO) 2.92 (4H, t, J = 6.1 Hz, $COCH_2$), 3.91 (4H, t, J = 6.1 Hz, CH_2Cl), 8.05 (2H, dd, J = 8.5 and 2.0 Hz, H-3,6), 8.17 (2H, d, J = 8.5 Hz, H-4,5), 8.48 (2H, d, J = 2.0 Hz, H-1,8), 10.72 (2H, s, NH); MS (rel intensity) m/z 419 (97), 355 (78), 329 (100), 307 (77), 289 (76), 254 (73), 232 (67), 214 (27); calcd ([M + 1]$^+$) 419.0565, found 419.0550. Anal. ($C_{20}H_{16}N_2O_4Cl_2 \cdot 0.25H_2O$) C, H, N, Cl.

1,5-Bis(3-piperidinopropionamido)anthracene-9,10-dione, 10a. General Aminolysis Procedure. To a stirred refluxing suspension of 1,5-bis(3-chloropropionamido)anthracene-9,10-dione (**6**) (1.00 g, 2.4 mmol) and NaI (0.3 g) in EtOH (40 mL) was added dropwise piperidine (3.0 mL, 30 mmol) in EtOH (10 mL). The mixture was stirred at reflux for 3 h, cooled to 0 °C, filtered, and washed with ether (50 mL). The crude solid was dissolved in hot $CHCl_3$ (200 mL), treated with decolorizing charcoal, and filtered. The filtrate was washed with water, dried, and evaporated to yield an orange solid. Recrystallization from DMF−EtOH (9:1 v/v) afforded amide **10a** (1.1 g, 89%) as orange needles: mp 214−215 °C; NMR δ ($CDCl_3$) 1.47 (4H, m, $(CH_2CH_2)_2CH_2$), 1.63 (8H, m, $N(CH_2CH_2)_2$), 2.52 (8H, t, J = 5.0 Hz, $N(CH_2CH_2)_2$), 2.72 (4H, m, $COCH_2CH_2$), 2.86 (4H, m, $COCH_2$), 7.76 (2H, t, J = 8.0 Hz, H-3,7), 8.03 (2H, dd, J = 8.0 and 1.0 Hz, H-4,8), 9.10

(2H, dd, J = 8.0 and 1.0 Hz, H-2,6), 12.31 (2H, s, NH); MS (rel intensity) m/z 517 (100), 516 (7), 307 (43), 289 (40), 246 (100), 207 (22); calcd ([M + 1]$^+$) 517.2815, found 517.2825. Anal. ($C_{30}H_{36}N_4O_4$) C, H, N. Diacetate salt: mp 215 °C. Dimethiodide salt **15a**: mp 230 °C dec. Anal. ($C_{32}H_{42}N_4O_4I_2\cdot H_2O$) C, H, N, I.

1,5-Bis(3-pyrrolidinopropionamido)anthracene-9,10-dione, 10b. Chloroamide **6** was treated with pyrrolidine according to the general aminolysis procedure to give amide **10b** (1.4 g, 80%) as yellow/orange needles: mp 194−195 °C; NMR δ ($CDCl_3$) 1.85 (8H, m, $N(CH_2CH_2)_2$), 2.66 (8H, m, $N(CH_2CH_2)_2$), 2.76 (4H, t, J = 7.6 Hz, $COCH_2CH_2$), 2.96 (4H, t, J = 7.6 Hz, $COCH_2$), 7.77 (2H, t, J = 8.0 Hz, H-3,7), 8.04 (2H, d, J = 8.0 Hz, H-4,8), 9.13 (2H, d, J = 8.0 Hz, H-2,6), 12.39 (2H, s, NH); MS (rel intensity) m/z 489 (100), 488 (39); calcd ([M + 1]$^+$) 489.2502, found 489.2512. Anal. ($C_{28}H_{32}N_4O_4$) C, H, N. Diacetate salt: mp 135−136 °C. Dimethiodide salt **15b**: mp 238 °C dec. Anal. ($C_{30}H_{38}N_4O_4I_2\cdot H_2O$) C, H, N, I.

1,5-Bis(3-morpholinopropionamido)anthracene-9,10-dione, 10c. Chloroamide **6** was treated with morpholine according to the general aminolysis procedure to give amide **10c** (1.6 g, 85%) as yellow needles: mp 268 °C; NMR δ ($CDCl_3$) 2.59 (8H, m, $N(CH_2CH_2)_2O$), 2.72 (4H, t, J = 6.0 Hz, $COCH_2CH_2$), 2.89 (4H, t, J = 6.0 Hz, $COCH_2$), 3.76 (8H, t, J = 4.6 Hz, $N(CH_2CH_2)_2O$), 7.79 (2H, t, J = 8.0 Hz, H-3,7), 8.04 (2H, d, J = 8.0 Hz, H-4,8), 9.11 (2H, d, J = 8.0 Hz, H-2,6), 12.37 (2H, s, NH); MS (rel intensity) m/z 521 (100), 520 (30); calcd ([M + 1]$^+$) 521.2400, found 521.2410. Anal. ($C_{28}H_{32}N_4O_6$) C, H, N. Diacetate salt: mp 266 °C. Dimethiodide salt **15c**: mp 245 °C dec. Anal. ($C_{30}H_{38}N_4O_6I_2$) C, H, N.

1,5-Bis[3-(dimethylamino)propionamido]anthracene-9,10-dione, 10d. Chloroamide **6** was treated with dimethylamine (10 mL of a 5.6 M solution in EtOH) according to the general aminolysis procedure to give amide **10d** (1.30 g, 83%) as yellow needles: mp 176−177 °C; NMR δ ($CDCl_3$) 2.36 (12H, s, CH_3), 2.69 (4H, m, $COCH_2CH_2$), 2.84 (4H, m, $COCH_2$), 7.77 (2H, t, J = 8.0 Hz, H-3,7), 8.04 (2H, d, J = 8.0 Hz, H-4,8), 9.14 (2H, d, J = 8.0 Hz, H-2,6), 12.39 (2H, s, NH); MS (rel intensity) m/z 437 (100), 436 (27), 307 (30), 289 (17); calcd ([M + 1]$^+$) 437.2189, found 437.2179. Anal. ($C_{24}H_{28}N_4O_4$) C, H, N. Diacetate salt: mp 142−143 °C. Dimethiodide salt **15d**: mp 250 °C dec. Anal. ($C_{26}H_{34}N_4O_4I_2\cdot 0.5H_2O$) C, H, N.

1,5-Bis[3-(diethylamino)propionamido]anthracene-9,10-dione, 10e. Chloroamide **6** was treated with diethylamine according to the general aminolysis procedure to give amide **10e** (1.28 g, 72%) as orange crystals: mp 174−175 °C; NMR δ ($CDCl_3$) 1.08 (12H, t, J = 7.0 Hz, CH_3), 2.65 (12H, m, J = 7.0 Hz, NCH_2), 2.97 (4H, t, J = 7.0 Hz, $COCH_2$), 7.76 (2H, t, J = 8.0 Hz, H-3,7), 8.04 (2H, d, J = 8.0 Hz, H-4,8), 9.13 (2H, d, J = 8.0 Hz, H-2,6), 12.33 (2H, s, NH); MS (rel intensity) m/z 493 (100), 492 (36); calcd ([M + 1]$^+$) 493.2815, found 493.2825. Anal. ($C_{28}H_{36}N_4O_4\cdot 0.5H_2O$) C, H, N. Diacetate salt: mp 91 °C. Dimethiodide salt **15e**: mp 235 °C dec. Anal. ($C_{30}H_{42}N_4O_4I_2\cdot 0.5H_2O$) C, H, N; I: calcd, 32.31; found, 33.01.

1,8-Bis(3-piperidinopropionamido)anthracene-9,10-dione, 11a. 1,8-Bis(3-chloropropionamido)anthracene-9,10-dione (**7**) (1.50 g, 3.6 mmol) was treated with piperidine according to the general aminolysis procedure to give amide **11a** (1.64 g, 89%) as yellow needles: mp 183−184 °C; NMR δ ($CDCl_3$) 1.50 (4H, m, $(CH_2CH_2)_2CH_2$), 1.65 (8H, m, $N(CH_2CH_2)_2$), 2.57 (8H, m, $N(CH_2CH_2)_2$), 2.83 (4H, t, J = 5.6 Hz, $COCH_2CH_2$), 2.88 (4H, t, J = 5.6 Hz, $COCH_2$), 7.77 (2H, t, J = 8.0 Hz, H-3,6), 8.05 (2H, dd, J = 8.0 and 1.0 Hz, H-4,5), 9.12 (2H, dd, J = 8.0 and 1.0 Hz, H-2,7), 12.11 (2H, s, NH); MS (rel intensity) m/z 517 (31), 431 (14), 405 (9), 376 (32), 347 (14), 292 (10), 265 (8), 238 (17), 138 (100), 112 (32); calcd ([M + 1]$^+$) 517.2815, found 517.2830. Anal. ($C_{30}H_{36}N_4O_4\cdot 1.2H_2O$) C, H, N. Diacetate salt: mp 174−176 °C. Dimethiodide salt **16a**: mp 244 °C dec. Anal. ($C_{32}H_{42}N_4O_4I_2\cdot 2.5H_2O$) C, N, I; H: calcd, 5.60; found, 5.03.

1,8-Bis(3-pyrrolidinopropionamido)anthracene-9,10-dione, 11b. Chloroamide **7** was treated with pyrrolidine according to the general aminolysis procedure to give amide **11b** (1.07 g, 61%) as yellow needles: mp 184−186 °C; NMR δ ($CDCl_3$) 1.84 (8H, m, $N(CH_2CH_2)_2$), 2.67 (8H, m, $N(CH_2CH_2)_2$), 2.80 (4H, m, $COCH_2CH_2$), 2.99 (4H, m, $COCH_2$), 7.77 (2H, t, J = 8.0 Hz, H-3,6), 8.05 (2H, d, J = 8.0 Hz, H-4,5), 9.14 (2H, d, J = 8.0 Hz, H-2,7), 12.17 (2H, s, NH); MS (rel intensity) m/z 489 (9), 417 (10), 391 (8), 362 (19), 347 (18), 292 (13), 238 (19), 155 (17), 124 (100); calcd ([M + 1]$^+$) 489.2502, found 489.2520. Anal. ($C_{28}H_{32}N_4O_4$) C, H, N. Diacetate salt: mp 179−180 °C. Dimethiodide salt **16b**: mp 228−230 °C dec. Anal. ($C_{30}H_{38}N_4O_4I_2\cdot 2H_2O$) C, H, N, I.

1,8-Bis(3-morpholinopropionamido)anthracene-9,10-dione, 11c. Chloroamide **7** was treated with morpholine according to the general aminolysis procedure except the mixture was heated at reflux for 24 h to give amide **11c** (1.82 g, 97%) as an orange solid: mp 230 °C; NMR δ ($CDCl_3$) 2.58 (8H, t, J = 4.4 Hz, $N(CH_2CH_2)_2O$), 2.75 (4H, t, J = 6.6 Hz, $COCH_2CH_2$), 2.88 (4H, t, J = 6.6 Hz, $COCH_2$), 3.74 (8H, t, J = 4.4 Hz, $N(CH_2CH_2)_2O$), 7.76 (2H, t, J = 7.8 Hz, H-3,6), 8.04 (2H, dd, J = 7.8 and 1.0 Hz, H-4,5), 9.13 (2H, dd, J = 7.8 and 1.0 Hz, H-2,7), 12.05 (2H, s, NH); MS (rel intensity) m/z 521 (100), 329 (12), 307 (45), 289 (27); calcd ([M + 1]$^+$) 521.2400, found 521.2420. Anal. ($C_{28}H_{32}N_4O_6$) C, H, N. Maleate salt: mp 190−192 °C. Dimethiodide salt **16c**: mp 232−233 °C dec. Anal. ($C_{30}H_{38}N_4O_6I_2\cdot 2H_2O$) C, H, N.

1,8-Bis[3-(dimethylamino)propionamido]anthracene-9,10-dione, 11d. Chloroamide **7** was treated with dimethylamine (10 mL of a 5.6 M solution in EtOH) according to the general aminolysis procedure to give amide **11d** (1.20 g, 76%) as orange needles: mp 126 °C; NMR δ ($CDCl_3$) 2.36 (12H, s, CH_3), 2.70 (4H, m, $COCH_2CH_2$), 2.80 (4H, m, $COCH_2$), 7.75 (2H, t, J = 8.0 Hz, H-3,6), 8.03 (2H, dd, J = 8.0 and 1.0 Hz, H-4,5), 9.13 (2H, dd, J = 8.0 and 1.0 Hz, H-2,7), 12.19 (2H, s, NH); MS (rel intensity) m/z 437 (100), 365 (15), 338 (15); calcd ([M + 1]$^+$) 437.2189, found 437.2170. Anal. ($C_{24}H_{28}N_4O_4$) C, H, N. Maleate salt: mp 188−189 °C. Dimethiodide salt **16d**: mp 263 °C dec. Anal. ($C_{26}H_{34}N_4O_4I_2\cdot H_2O$) C, H, N.

1,8-Bis[3-(diethylamino)propionamido]anthracene-9,10-dione, 11e. Chloroamide **7** was treated with diethylamine according to the general aminolysis procedure to give amide **11e** (1.58 g, 89%) as orange crystals: mp 175−176 °C; NMR δ ($CDCl_3$) 1.08 (12H, t, J = 7.0 Hz, CH_3), 2.66 (12H, m, J = 7.0 Hz, NCH_2), 2.97 (4H, t, J = 7.0 Hz, $COCH_2$), 7.75 (2H, t, J = 8.0 Hz, H-3,6), 8.04 (2H, dd, J = 8.0 and 1.0 Hz, H-4,5), 9.13 (2H, dd, J = 8.0 and 1.0 Hz, H-2,7), 12.11 (2H, s, NH); MS (rel intensity) m/z 493 (100), 307 (28), 289 (18); calcd ([M + 1]$^+$) 493.2815, found 493.2800. Anal. ($C_{28}H_{36}N_4O_4\cdot 3.75H_2O$) C, N; H: calcd, 7.83; found, 6.40. Maleate salt: mp 149−150 °C. Dimethiodide salt **16e**: mp 218−220 °C. Anal. ($C_{30}H_{42}N_4O_4I_2\cdot 6H_2O$) C, N; H: calcd, 6.15; found, 4.83; I: calcd, 28.69; found, 28.24.

2,7-Bis(3-piperidinopropionamido)anthracene-9,10-dione, 13a. 2,7-Bis(3-chloropropionamido)anthracene-9,10-dione (**8**) was treated with piperidine according to the general aminolysis procedure to give amide **13a** (1.85 g, 99%) as a pale-yellow solid: mp 240 °C dec; NMR δ (DMSO) 1.40 (4H, m, $(CH_2CH_2)_2CH_2$), 1.51 (8H, m, $N(CH_2CH_2)_2$), 2.42 (8H, m, $N(CH_2CH_2)_2$), 2.56 (4H, t, J = 5.8 Hz, $COCH_2CH_2$), 2.65 (4H, t, J = 5.8 Hz, $COCH_2$), 8.04 (2H, dd, J = 8.5 and 2.0 Hz, H-3,6), 8.15 (2H, d, J = 8.5 Hz, H-4,5), 8.45 (2H, d, J = 2.0 Hz, H-1,8), 10.80 (2H, s, NH); MS (rel intensity) m/z 517 (100), 329 (12), 307 (43), 289 (25), 259 (11); calcd ([M + 1]$^+$) 517.2815, found 517.2840. Anal. ($C_{30}H_{36}N_4O_4\cdot 0.5H_2O$) C, H, N. Maleate salt: mp 138−140 °C. Dimethiodide salt **18a**: mp 192−193 °C dec. Anal. ($C_{32}H_{42}N_4O_4I_2$) C, H, N.

2,7-Bis(3-pyrrolidinopropionamido)anthracene-9,10-dione, 13b. Chloroamide **8** was treated with pyrrolidine according to the general aminolysis procedure to give amide **13b** (1.68 g, 95%) as a pale-yellow solid: mp 232 °C dec; NMR δ (DMSO) 1.69 (8H, m, $N(CH_2CH_2)_2$), 2.49 (8H, m, $N(CH_2CH_2)_2$), 2.56 (4H, t, J = 6.5 Hz, $COCH_2CH_2$), 2.76 (4H, t, J = 6.5 Hz, $COCH_2$), 8.04 (2H, d, J = 8.5 Hz, H-3,6), 8.15 (2H, d, J = 8.5 Hz, H-4,5), 8.45 (2H, s, H-1,8), 10.65 (2H, s, NH); MS (rel intensity) m/z 489 (100), 307 (20), 289 (12); calcd ([M + 1]$^+$) 489.2502, found 489.2520. Anal. ($C_{28}H_{32}N_4O_4\cdot 0.5H_2O$) C,

H, N. Maleate salt: mp 172−174 °C dec. Dimethiodide salt **18b**: mp 216−218 °C dec. Anal. ($C_{30}H_{38}N_4O_4I_2$) C, H, N.

2,7-Bis(3-morpholinopropionamido)anthracene-9,10-dione, 13c. Chloroamide **8** was treated with morpholine according to the general aminolysis procedure except the mixture was heated at reflux for 5 h to give amide **13c** (1.86 g, 99%) as a pale-yellow solid: mp 235 °C dec; NMR δ (DMSO) 2.43 (8H, m, N(CH_2CH_2)$_2$O), 2.58−2.67 (8H, m, COCH_2CH_2), 3.58 (8H, m, N(CH_2CH_2)$_2$O), 8.05 (2H, dd, J = 8.5 and 2.1 Hz, H-3,6), 8.15 (2H, d, J = 8.5 Hz, H-4,5), 8.47 (2H, d, J = 2.1 Hz, H-1,8), 10.71 (2H, s, NH); MS (rel intensity) m/z 521 (100), 329 (19), 307 (73), 289 (42); calcd ([M + 1]$^+$) 521.2400, found 521.2420. Anal. ($C_{28}H_{32}N_4O_6\cdot0.75H_2O$) C, N; H: calcd, 6.32; found, 5.89. Maleate salt: mp 130−135 °C dec. Dimethiodide salt **18c**: mp 238 °C dec. Anal. ($C_{30}H_{38}N_4O_6I_2$) C, H, N.

2,7-Bis[3-(dimethylamino)propionamido]anthracene-9,10-dione, 13d. Chloroamide **8** (1.50 g, 3.6 mmol) was treated with dimethylamine (10 mL of a 5.6 M solution in EtOH) according to the general aminolysis procedure to give amide **13d** (1.48 g, 94%) as a pale-yellow solid: mp 202−203 °C; NMR δ (DMSO) 2.18 (12H, s, CH_3), 2.55 (8H, m, COCH_2CH_2), 8.05 (2H, d, J = 9.0 Hz, H-3,6), 8.15 (2H, d, J = 9.0 Hz, H-4,5), 8.46 (2H, s, H-1,8), 10.68 (2H, s, NH); MS (rel intensity) m/z 437 (100), 329 (11), 307 (42), 289 (22); calcd ([M + 1]$^+$) 437.2189, found 437.2170. Anal. ($C_{24}H_{28}N_4O_4\cdot1.25H_2O$) C, H, N. Maleate salt: mp 167−169 °C dec. Dimethiodide salt **18d**: mp 223−224 °C. Anal. ($C_{26}H_{34}N_4O_4I_2\cdot0.75H_2O$) C, H, N.

2,7-Bis[3-(diethylamino)propionamido]anthracene-9,10-dione, 13e. Chloroamide **8** was treated with diethylamine according to the general aminolysis procedure to give amide **13e** (1.56 g, 88%) as a pale-yellow solid: mp 215 °C; NMR δ (DMSO) 0.98 (12H, t, J = 7.1 Hz, CH_3), 2.50 (12H, qt, J = 7.1 and 7.0 Hz, NCH_2), 2.78 (4H, t, J = 7.0 Hz, $COCH_2$), 8.04 (2H, dd, J = 8.5 and 2.1 Hz, H-3,6), 8.15 (2H, d, J = 8.5 Hz, H-4,5), 8.45 (2H, d, J = 2.1 Hz, H-1,8), 10.75 (2H, s, NH); MS (rel intensity) m/z 493 (100), 477 (12); calcd ([M + 1]$^+$) 493.2815, found 493.2800. Anal. ($C_{28}H_{36}N_4O_4\cdot0.25H_2O$) C, H, N. Maleate salt: mp 154−156 °C. Dimethiodide salt **18e**: mp 196 °C. Anal. ($C_{30}H_{42}N_4O_4I_2$) H, N; C: calcd, 46.40; found, 47.61.

Biological Studies. 1. *Taq* Polymerase Assay. Compounds (acid addition and quaternary dimethiodide salts) were tested at 10, 20, and 50 μM final concentrations in a PCR 50-μL master mix containing 10 ng of pCI-neo mammalian expression vector (Promega, Southampton, U.K.) and forward (GGAGTTCCGCGTTACATAAC) and reverse (GTCTGCTCGAAGCATTAACC) primers (200 nmol) as described previously.[17] The product of approximately 1 kb was visualized on a 2% w/w agarose gel following amplification (30 cycles of 94 °C for 1 min, 55 °C for 1 min, and 72 °C for 2.5 min).

2. Modified Telomeric Repeat Amplification Protocol (TRAP) Assay. The ability of agents to inhibit telomerase in a cell-free assay was assessed with a modified TRAP assay using extracts from exponentially growing A2780 human ovarian carcinoma cells as described previously.[17] The TRAP assay was performed in two steps: (a) Telomerase-mediated extension of the forward primer (TS: 5′-AATCCGTCGAGCAGAGTT; Oswel Ltd., Southampton, U.K.) was contained in a 40-μL reaction mix comprising TRAP buffer (20 mM Tris-HCl (pH 8.3), 68 mM KCl, 1.5 mM $MgCl_2$, 1 mM EGTA, 0.05% v/v Tween 20), 0.05 μg of bovine serum albumin, 50 μM of each deoxynucleotide triphosphate, 0.1 μg of TS primer, and 3 μCi of [α-^{32}P]dCTP (Amersham plc, U.K.). Protein (0.04 μg) was then incubated with the reaction mix ± agent (acid addition and quaternary dimethiodide salts) at final concentrations of up to 50 μM for 20 min at 25 °C. A lysis buffer (no protein) control, heat-inactivated protein control, and 50% protein (0.02 μg) control were included in each assay. (b) While heating at 80 °C in a PCR block of a thermal cycler (Hybaid, U.K.) for 5 min to inactivate telomerase activity, 0.1 μg of reverse CX primer (3′-AATCCCATTCCCATTCCCATTCCC-5′) and 2 units of *Taq* DNA polymerase ("red hot"; Advanced Biotechnologies) were added. A three-step PCR was then performed: 94 °C for 30 s, 50 °C for 30 s, and 72 °C for 1 min for 31 cycles. Telomerase-extended PCR products in the presence or absence of compounds were then determined either by electrophoretic separation using 8% w/w acrylamide denaturing gels and analysis by phosphorimaging or autoradiography or by harvesting on Whatman filters (25-mm glass microfiber) and analysis by liquid scintillation counting.

3. Growth Inhibition Assay. Growth inhibition was measured in three human ovarian carcinoma cell lines (A2780, CH1, and SKOV-3) using the sulforhodamine B (SRB) assay as described previously.[26] Briefly, between 3000 and 6000 cells were seeded into the wells of 96-well microtiter plates and allowed to attach overnight. Agents (acid addition and quaternary dimethiodide salts) were dissolved at 500 μM in water and immediately added to wells in quadruplicate at final concentrations of 0.05, 0.25, 1, 5, and 25 μM. Following an incubation period of 96 h, remaining cells were fixed with ice-cold 10% w/v trichloroacetic acid (30 min) and stained with 0.4% SRB in 1% v/v acetic acid (15 min). Mean absorbance at 540 nm for each drug concentration was expressed as a percentage of the control untreated well absorbance, and IC_{50} values (concentration required to inhibit cell growth by 50%) were determined for each agent.

4. Isothermal Titration Calorimetry. Calorimetric experiments were carried out using the isothermal titration module of a Microcal MCS high-sensitivity titration calorimeter (Microcal Inc., Northampton, MA). Data acquisition and analysis were performed using the Origin 4.10 software package (supplied by the manufacturer). All experiments were conducted at 25.00 ± 0.01 °C in aqueous buffer (10 mM Tris-HCl, 150 mM KCl, pH 7.0). The human telomeric DNA sequence d[$AG_3(T_2AG_3)_3$] was purchased from Oswel Ltd. (Southampton, U.K.) and was used without further purification. Binding isotherms were determined by serial 5-μL injections of ligand solution (1.4 mM) at 400-s intervals from a 250-μL syringe rotating at 400 rpm into DNA solution (37 μM). The raw calorimetric data were integrated and corrected for sample concentration and cell volume affording the heat output per injection. Control experiments were performed to determine the heats of dilution for ligand titrated into buffer, and the binding isotherm for each ligand−DNA interaction was calculated by subtraction of the heat of dilution.[25] The binding enthalpy ($\Delta H°$), equilibrium binding constant (K_b), and stoichiometry (n) for each ligand−DNA interaction were determined from the corrected binding isotherms using a nonlinear least-squares fitting procedure.

5. Molecular Modeling Studies. The Macromodel 5.0 program[40] using the AMBER* force field with continuum solvation treatment (GB/SA model of water solvation, van der Waals cutoff 8 Å, electrostatic cutoff 20 Å, dielectric constant 1) was used for all model building and calculations. The solution NMR structure of the human telomeric repeat d[$AG_3(T_2AG_3)_3$] G-quadruplex[11] was modeled to give an initial low-energy starting model. Molecular mechanics energy minimization (1000-steps steepest descent with line searching and 3000-steps Polak Ribiere conjugate gradient with derivative convergence of 0.05 kJ/Å mol) followed by dynamics (1.5-fs time step, 40 ps at 300 K equilibrium, 100 ps at 300 K production with time averaging of 100 sampled structures) and subsequent mechanics (minimization of time-averaged dynamics structure) was used. An intercalation site was introduced between the diagonal T_2A loop and the G-quartet segment of the structure (5′-AG step) by breaking the phosphate backbones and separating the structure while monitoring the distance between the segments. The sugar−phosphate chains were reconnected, and molecular mechanics energy minimization (1000-steps steepest descent with line searching followed by 1000-steps conjugate gradient) was used to relieve any resulting steric distortion while retaining the G-quartet and loop motifs with positional restraints.

Models of the five regioisomeric piperidine derivatives were built and energy-minimized using the same procedure as described for the phosphate backbones. The minimized anthraquinones were, in turn, docked into the intercalation site,

and different positions of the chromophore were systematically evaluated for each regioisomer. Selections were made on the basis of maximization of π-electron overlap between the G-quartet, the chromophore, and the adenine pair. Where necessary, alterations to the conformation of the $-(CH_2)_2-$ side chain linkers were made to alleviate any intermolecular clashes.

The resulting G-quadruplex−ligand complexes were minimized using molecular mechanics (1000-steps steepest descent with line searching and 3000-steps Polak Ribiere conjugate gradient with derivative convergence of 0.05 kJ/Å mol) followed by dynamics (1.5-fs time step, 100 ps at 300 K equilibrium, 100 ps at 300 K production with time averaging of 100 sampled structures) and subsequent mechanics (minimization of time-averaged dynamics structure). No positional restraints were placed on any part of the model during these calculations.

Acknowledgment. This work was supported by the Cancer Research Campaign and Institute of Cancer Research. Paul Rogers is thanked for conducting cytotoxicity assays. We gratefully thank Heath Scientific for their expert guidance and use of ITC instrumentation for thermodynamic experiments.

References

(1) (a) Morin, G. B. Is Telomerase a Universal Cancer Target? *J. Natl. Cancer Inst.* **1995**, *87*, 859−861. (b) Hamilton, S. E.; Corey, D. R. Telomerase: Anti-cancer Target or just a Fascinating Enzyme? *Chem. Biol.* **1996**, *3*, 863−867. (c) Parkinson, E. K. Do Telomerase Antagonists Represent a Novel Anti-cancer Strategy? *Br. J. Cancer* **1996**, *73*, 1−4. (d) Raymond, E.; Sun, D.; Chen, S.-F.; Windle, B.; von Hoff, D. D. Agents that Target Telomerase and Telomeres. *Curr. Opin. Biotechnol.* **1996**, *7*, 583−591.

(2) (a) Bodnar, A. G.; Ouellette, M.; Frolkis, M.; Holt, S. E.; Chiu, C. P.; Morin, G. B.; Harley, C. B.; Shay, J. W.; Lichtsteiner, S.; Wright, W. E. Extension of Life-span by Introduction of Telomerase into Normal Human Cells. *Science* **1998**, *279*, 349−352. (b) Niida, H.; Matsumoto, T.; Satoh, H.; Shiwa, M.; Tokutake, Y.; Furuichi, Y.; Shinkai, Y. Severe Growth Defect in Mouse Cells Lacking the Telomerase RNA Component. *Nature Genet.* **1998**, *19*, 203−206.

(3) (a) Morin, G. B. The Human Telomere Terminal Transferase Activity is a Ribonucleoprotein that Synthesises TTAGGG Repeats. *Cell* **1989**, *59*, 521−529. (b) Feng, J.; Funk, W.; Wang, S.-S.; Weinrich, S. L.; Avilion, A. A.; Chiu, C.-P.; Adams, R. R.; Chang, E.; Allsopp, R. C.; Yu, J.; Le, S.; West, M. D.; Harley, C. B.; Andrews, W. H.; Greider, C. W.; Villeponteau, B. The RNA Component of Human Telomerase. *Science* **1995**, *269*, 1236−1241.

(4) Blackburn, E. H. Structure and Function of Telomeres. *Nature* **1991**, *350*, 569−573.

(5) Meyne, J.; Ratliff, R. L.; Moyzis, R. K. Conservation of the Human Telomere Sequence $(TTAGGG)_n$ among Vertebrates. *Proc. Natl. Acad. Sci. U.S.A.* **1989**, *86*, 7049−7053.

(6) Blackburn, E. H. Telomeres: No End in Sight. *Cell* **1994**, *77*, 621−623.

(7) Kruk, P. A.; Rampino, N. J.; Bohr, V. A. DNA Damage and Repair in Telomeres: Relation to Aging. *Proc. Natl. Acad. Sci. U.S.A.* **1995**, *92*, 258−262.

(8) (a) Harley, C. B.; Futcher, A. B.; Greider, C. W. Telomeres Shorten During Aging of Human Fibroblasts. *Nature* **1990**, *345*, 458−460. (b) Allsopp, R. C.; Harley, C. B. Evidence for a Critical Telomere Length in Senescent Human Fibroblasts. *Exp. Cell Res.* **1995**, *219*, 130−136.

(9) Kim, N. W.; Piatyszek, M. A.; Prowse, K. R.; Harley, C. B.; West, M. D.; Ho, P. L. C.; Coviello, G. M.; Wright, W. E.; Weinrich, R. L.; Shay, J. W. Specific Association of Human Telomerase Activity with Immortal Cells and Cancer. *Science* **1994**, *266*, 2011−2015.

(10) Counter, C. M.; Hirte, H. W.; Bacchetti, S.; Harley, C. B. Telomerase Activity in Human Ovarian Carcinoma. *Proc. Natl. Acad. Sci. U.S.A.* **1994**, *91*, 2900−2904.

(11) Wang, Y.; Patel, D. J. Solution Structure of the Human Telomeric Repeat $d[AG_3(T_2AG_3)_3]$ G-tetraplex. *Structure* **1993**, *1*, 263−282.

(12) Williamson, J. R. G-quartet Structures in Telomeric DNA. *Annu. Rev. Biophys. Biomol. Struct.* **1994**, *23*, 703−730.

(13) Rhodes, D.; Giraldo, R. Telomere Structure and Function. *Curr. Opin. Struct. Biol.* **1995**, *5*, 311−322.

(14) Zahler, A. M.; Williamson, J. R.; Cech, T. R.; Prescott, D. M. Inhibition of Telomerase by G-quartet DNA Structures. *Nature* **1991**, *350*, 718−720.

(15) Fletcher, T. M.; Sun, D.; Salazar, M.; Hurley, L. H. Effect of DNA Secondary Structure on Human Telomerase Activity. *Biochemistry* **1998**, *37*, 5536−5541.

(16) Sun, D.; Thompson, B.; Cathers, B. E.; Salazar, M.; Kerwin, S. M.; Trent, J. O.; Jenkins, T. C.; Neidle, S.; Hurley, L. H. Inhibition of Human Telomerase by a G-Quadruplex-Interactive Compound. *J. Med. Chem.* **1997**, *40*, 2113−2116.

(17) Perry, P. J.; Gowan, S. M.; Reszka, A. P.; Polucci, P.; Jenkins, T. C.; Kelland, L. R.; Neidle, S. 1,4- and 2,6-Disubstituted Amidoanthracene-9,10-dione Derivatives as Inhibitors of Human Telomerase. *J. Med. Chem.* **1998**, *41*, 3253−3260.

(18) Wheelhouse, R.; Sun, D.; Han, H.; Han, F. X.; Hurley, L. H. Cationic Porphyrins as Telomerase Inhibitors: the Interaction of Tetra-(*N*-methyl-4-pyridyl)porphine with Quadruplex DNA. *J. Am. Chem. Soc.* **1998**, *120*, 3261−3262.

(19) Anantha, N. V.; Azam, M.; Sheardy, R. D. Porphyrin Binding to Quadruplexed T_4G_4. *Biochemistry* **1998**, *37*, 2709−2714.

(20) Collier, D. A.; Neidle, S. Synthesis, Molecular Modeling, DNA Binding, and Antitumor Properties of Some Substituted Amidoanthraquinones. *J. Med. Chem.* **1988**, *31*, 847−857.

(21) Agbandje, M.; Jenkins, T. C.; McKenna, R.; Reszka, A. P.; Neidle, S. Anthracene-9,10-diones as Potential Anticancer Agents. Synthesis, DNA-Binding, and Biological Studies on a Series of 2,6-Disubstituted Derivatives. *J. Med. Chem.* **1992**, *35*, 1418−1429.

(22) Tanious, F. A.; Jenkins, T. C.; Neidle, S.; Wilson, W. D. Substituent Position Dictates the Intercalative DNA-Binding Mode for Anthracene-9,10-dione Antitumor Drugs. *Biochemistry* **1992**, *31*, 11632−11640.

(23) Neidle, S.; Jenkins, T. C. Molecular Modeling to Study DNA Intercalation by Antitumor Drugs. *Methods Enzymol.* **1991**, *203*, 433−459.

(24) Fox, K. R.; Polucci, P.; Jenkins, T. C.; Neidle, S. A Molecular Anchor for Stabilizing Triple-Helical DNA. *Proc. Natl. Acad. Sci. U.S.A.* **1995**, *92*, 7887−7891.

(25) Haq, I.; Ladbury, J. E.; Chowdhry, B. Z.; Jenkins, T. C. Molecular Anchoring of Duplex and Triplex DNA by Disubstituted Anthracene-9,10-diones: Calorimetric, UV Melting and Competition Dialysis Studies. *J. Am. Chem. Soc.* **1996**, *118*, 10693−10701.

(26) Kelland, L. R.; Abel, G.; McKeage, M. J.; Jones, M.; Goddard, P. M.; Valenti, M.; Murrer, B. A.; Harrap, K. R. Preclinical Antitumor Evaluation of Bis-acetato-amine-dichloro-cyclohexylamine Platinum(IV): an Orally Active Platinum Drug. *Cancer Res.* **1993**, *53*, 2581−2586.

(27) (a) Strahl, C.; Blackburn, E. H. Effects of Reverse Transcriptase Inhibitors on Telomere Length and Telomerase Activity in Two Immortalised Human Cell Lines. *Mol. Cell. Biol.* **1996**, *16*, 53−65. (b) Yegorov, Y. E.; Chernov, D. N.; Akimov, S. S.; Bolsheva, N. L.; Krayevsky, A. A.; Zelenin, A. V. Reverse Transcriptase Inhibitors Suppress Telomerase Function and Induce Senescence-like Processes in Cultured Mouse Fibroblasts. *FEBS Lett.* **1996**, *389*, 115−118. (c) Melana, S. M.; Holland, J. F.; Pogo, B. G.-T. Inhibition of Cell Growth and Telomerase Activity of Breast Cancer Cells In Vitro by 3′-Azido-3′deoxythymidine. *Clin. Cancer Res.* **1944**, *4*, 693−696. (d) Fletcher, T. M.; Salazar, M.; Chen, S.-F. Human Telomerase Inhibition by 7-Deaza-2′-deoxypurine Nucleoside Triphosphates. *Biochemistry* **1996**, *35*, 15611−15617. (e) Pai, R. B.; Pai, B.; Kukhanova, M.; Dutschman, G. E.; Guo, X.; Cheng, Y.-C. Telomerase from Human Leukemia Cells: Properties and Its Interaction with Deoxynucleoside Analogues. *Cancer Res.* **1998**, *58*, 1909−1913.

(28) (a) Ku, W.-C.; Cheng, A.-J.; Wang, T.-C. V. Inhibition of Telomerase Activity by PKC Inhibitors in Human Nasopharyngeal Cancer Cells in Culture. *Biochem. Biophys. Res. Commun.* **1997**, *241*, 730−736. (b) Yamakuchi, M.; Nakata, M.; Kawahara, K.-I.; Kitajima, I.; Maruyama, I. New Quinolones, Ofloxacin and Levofloxacin, Inhibit Telomerase Activity in Transitional Cell Carcinoma Cell Lines. *Cancer Lett.* **1997**, *119*, 213−219.

(29) Guo, Q.; Lu, M.; Marky, L. A.; Kallenbach, N. R. Interaction of the Dye Ethidium Bromide with DNA Containing Guanine Repeats. *Biochemistry* **1992**, *31*, 2451−2455.

(30) O'Neill, C. F.; Orr, R. M.; Kelland, L. R.; Harrap, K. R. Comparison of Platinum Binding to DNA and Removal of Total Platinum Adducts and Inter-Strand Cross-Links in three Human Ovarian Carcinoma Cell Lines Sensitive and Resistant to Cisplatin. *Cell. Pharmacol.* **1995**, *2*, 1−7.

(31) Jenkins, T. C. Unpublished results.

(32) Blasco, M. A.; Lee, H.-W.; Hande, M. P.; Samper, E.; Lansdorp, P. M.; DePinho, R. A.; Greider, C. W. Telomere Shortening and Tumor Formation by Mouse Cells Lacking Telomerase RNA. *Cell* **1997**, *91*, 25−34.

(33) Lee, H.-W.; Blasco, M. A.; Gottlieb, G. J.; Horner, J. W.; Greider, C. W.; DePinho, R. A. Essential Role of Mouse Telomerase in Highly Proliferative Organs. *Nature* **1998**, *392*, 569−574.

(34) Kondo, S.; Kondo, Y.; Li, G.; Silverman, R. H.; Cowell, J. K. Targeted Therapy of Human Malignant Glioma in a Mouse Model by 2-5A Antisense Directed Against Telomerase RNA. *Oncogene* **1998**, *16*, 3323−3330.
(35) Bryan, T. M.; Englezou, A.; Dalla-Pozza, L.; Dunham, M. A.; Reddel, R. R. Evidence for an Alternative Mechanism for Maintaining Telomere Length in Human Tumors and Tumor-derived Cell Lines. *Nature Med.* **1997**, *3*, 1271−1274.
(36) Venitt, S.; Crofton-Sleigh, C.; Agbandje, M.; Jenkins, T. C.; Neidle, S. Anthracene-9,10-diones as Potential Anti-Cancer Agents: Bacterial Mutation Studies of Amido-Substituted Derivatives Reveal an Unexpected Lack of Mutagenicity. *J. Med. Chem.* **1998**, *41*, 3748−3752.
(37) House, H. O.; Koepsell, D. G.; Campbell, W. J. The Synthesis of Some Diphenyl and Triphenyl Derivatives of Anthracene and Naphthalene. *J. Org. Chem.* **1972**, *37*, 1003−1011.
(38) Böernstein, E.; Schliewiensky, H.; Szczesny-Heyl, G. V. Fritzsches Reagent: β-Dinitroanthraquinones. *Chem. Ber.* **1926**, *59*, 2813.
(39) Gubelmann, I.; Weiland, H. J.; Stallmann, O. Several New 4′-Sulfo-*ortho*-benzoylbenzoic Acid Derivatives and the Corresponding Anthraquinone Compounds. *J. Am. Chem. Soc.* **1931**, *53*, 1033−1036.
(40) Mohamadi, F.; Richards, N. G. J.; Guida, W. C.; Liskamp, R.; Lipton, M.; Caufield, C.; Chang, G.; Hendrickson, T.; Still, W. C. Macromodel − an Integrated Software System for Modeling Organic Bioorganic Molecules using Molecular Mechanics. *J. Comput. Chem.* **1990**, *11*, 440−467.

JM981067O